

# Partial coalescence between a drop and a liquid-liquid interface

Xiaopeng Chen

*Department of Chemical and Biological Engineering, University of British Columbia, Vancouver, British Columbia V6T 1Z3, Canada*

Shreyas Mandre

*Department of Mathematics, University of British Columbia, Vancouver, British Columbia V6T 1Z2, Canada*

James J. Feng<sup>a)</sup>

*Department of Chemical and Biological Engineering and Department of Mathematics, University of British Columbia, Vancouver, British Columbia V6T 1Z3, Canada*

(Received 16 December 2005; accepted 28 March 2006; published online 23 May 2006)

This Letter reports experimental results for partial coalescence when a drop merges with an interface. We find an intermediate range of drop sizes in which the merger is not complete but a daughter drop is left behind. This phenomenon is governed primarily by inertia and interfacial tension, and three regimes can be further delineated depending on the roles of viscosity and gravity. Scaling relationships are developed for the drop size ratio and the coalescence time. For drops that are too large or too small, partial coalescence is arrested by gravity or viscosity, respectively.

© 2006 American Institute of Physics. [DOI: [10.1063/1.2201470](https://doi.org/10.1063/1.2201470)]

Consider a drop falling through an ambient fluid and merging with an interface. If the drop and the lower bulk are of the same fluid (Fig. 1), a peculiar partial coalescence cascade has been documented. The drop first rests on a thin film of the ambient fluid trapped between the drop and the interface.<sup>1</sup> The film drains slowly until finally it ruptures at a point and the drop makes contact with the lower bulk phase. The fluid in the drop begins to merge with the bulk phase. This merger may not always be complete, but a smaller daughter drop may be left behind resulting in only a partial coalescence.<sup>2</sup> This process may repeat as many as eight times before the coalescence is complete.<sup>3</sup>

Four dimensionless numbers are important to this process: the Bond number  $Bo = (\rho_1 - \rho_2)gD^2/\sigma$ , the Ohnesorge number  $Oh = \mu_1/\sqrt{(\rho_1 + \rho_2)\sigma D}$ , the density ratio  $\rho_* = \rho_1/\rho_2$ , and the viscosity ratio  $\mu_* = \mu_1/\mu_2$ . Charles and Mason<sup>2</sup> and Mohamed-Kassim and Longmire<sup>4</sup> described the partial coalescence process as the propagation and focusing of capillary waves followed by Rayleigh instability. The latter authors also suggested a criterion for partial coalescence based on  $Bo\bar{Oh}$ , where  $\bar{Oh} = Oh(1 + \mu_*^{-1})/\sqrt{2}$ . For fluids of low viscosity, Thoroddsen and Takehara<sup>3</sup> identified a narrow intermediate range of drop diameters for which the viscous and gravitational forces are both negligible,  $Bo \rightarrow 0$ ,  $Oh \rightarrow 0$ . With ethanol drops coalescing with an air-ethanol interface, they observed a self-similar behavior in which the drop size is reduced by the same fraction in each cycle of partial coalescence.

This Letter reports recent experiments with low-viscosity fluids that expand our knowledge on the partial coalescence process to finite values of  $Bo$  and  $Oh$ . Besides the self-similar regime, we have identified two other regimes of partial coalescence that are strongly influenced, respec-

tively, by viscosity and gravity. For the self-similar regime, we adapt the idea of capillary wave propagation to explain the dependence of the coalescence time on fluid density. This was not examined by Thoroddsen and Takehara<sup>3</sup> whose ethanol-air system had a very large  $\rho_*$ . For the two new regimes, we derive scaling laws for the coalescence time and the size ratio between the daughter and mother drops. The bounds of the two regimes give rise to criteria for the occurrence of partial coalescence. Both the scaling laws and the criteria are representative of data from our experiments as well as from previous studies.

For the drop and lower bulk fluid, we have used water and water-glycerol mixtures. For the matrix fluid surrounding the drop, we have used decane with a varying amount of polybutene (molecular weight ~800, H-35 from BP Amoco) dissolved in it. The physical parameters of the different fluid pairs are given in Table I. By varying the glycerol and polybutene concentrations, we have explored ranges of the four dimensionless parameters defined above. The experimental setup consists of a container with the fluid interface, above which drops are formed using a syringe and a needle. The process of coalescence is recorded by a high-speed camera (model MS70K, Canadian Photonics Labs) at 4000 to 18 000 frames/sec.

We find that for partial coalescence to occur, the drop size has to be in a specific range. Within this range, we further define three regimes of partial coalescence with distinct characteristics, most prominently demonstrated by the coalescence time  $\tau_c$ , the interval between film rupture and pinchoff of the daughter drop (Fig. 2), and the diameter ratio  $\zeta$  between the daughter drop and the mother drop (Fig. 3). For each fluid pair, data are taken through the partial coalescence cascade as the drop diameter shrinks stepwise. The uncertainty in measuring the drop size is 1 pixel in a magnified image and that in measuring time depends on the frame speed. Error bars are indicated on one set of data (circles),

<sup>a)</sup>Author to whom correspondence should be addressed. Electronic mail: [jfeng@chml.ubc.ca](mailto:jfeng@chml.ubc.ca)

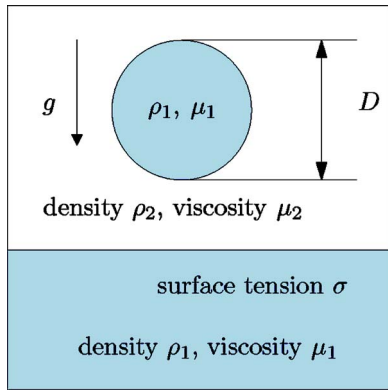


FIG. 1. Schematic of the partial coalescence process. The drop diameter ranges from  $40 \mu\text{m}$  to 3 mm, and the container is 5 cm diam.

and are representative of all sets. First, note the self-similar regime in the middle, where both  $\tau_c$  and  $\zeta$  are roughly independent of the drop size. In this regime, both gravity and viscosity are insignificant, and the dynamics is determined by the balance between capillarity and inertia. Thus, we may call this the inertio-capillary regime. For larger drops, Oh is smaller but Bo becomes important. We call this the gravitational regime. For smaller drops, Bo decreases further but viscous effects become significant as Oh increases. Thus we enter the viscous regime. In the gravitational regime, both  $\tau_c$  and  $\zeta$  decrease as the drop gets larger. In the viscous regime, the data are more scattered owing to the differing  $\mu_*$  among fluid pairs and to greater uncertainty in measuring shorter times for smaller drops. But  $\tau_c$  increases as the drop gets smaller, while  $\zeta$  tends to decrease before dropping precipitously to zero as the minimum size for partial coalescence is reached. While  $\text{Bo} \propto \text{Oh}^{-4}$  for each fluid pair, the proportionality constant differs for different fluid pairs. Thus there is no universal correspondence between Bo and Oh. In both figures we have plotted data against Bo in the gravitational and inertio-capillary regimes. The Oh values in this range serve only as a rough indication. In the viscous regime, similarly, data are plotted against Oh while the Bo values are inexact.

To understand the fluid dynamics of partial coalescence, we examine snapshots of one cycle of partial coalescence in Fig. 4. Although this cycle happens to be in the self-similar inertio-capillary regime, the salient features are universal among all three regimes. As indicated by previous experiments,<sup>2,4</sup> the process of partial coalescence can be divided into two stages: propagation of surface waves and cap-

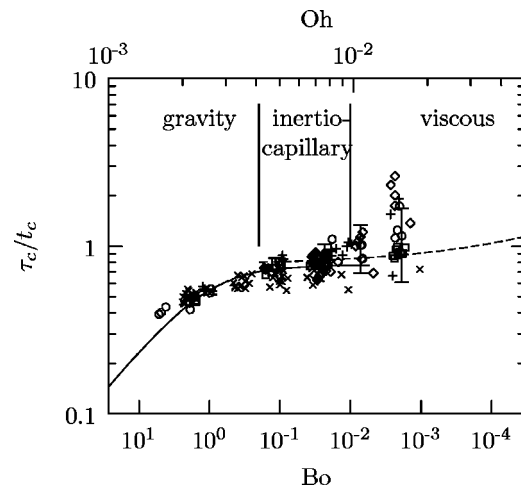


FIG. 2. The coalescence time scaled by the capillary time [Eq. (1)] as a function of Bo and Oh. The symbols represent various fluid combinations as listed in Table I; crosses are for ethanol in air (Ref. 3). The solid line is based on Eq. (2):  $\tau_c/t_c = 0.77(1+\text{Bo})^{-1/2}$ . The dashed line, based on Eq. (3):  $\tau_c/t_c = 0.77(1+9.68\text{Oh})$ , is a fitting for the pluses.

illary pinchoff. As the matrix film ruptures, the interface momentarily becomes singular<sup>5</sup> and the contact region expands rapidly. This sets off a surface capillary wave that propagates up the drop surface, as indicated by the arrows in Fig. 4. Of course, a similar surface wave propagates radially outward along the initially flat interface, but it has little relevance to partial coalescence. In the mean time, the drop fluid drains into the bulk because of the capillary pressure inside the drop and gravity. The capillary wave reaches the top of the drop after some time and imparts a vertical velocity to the interface there, lifting it upward. This effect is evident from the increased height of the liquid column in Fig. 4, and has been amplified by the focusing or collision of the waves at the center. While drainage at the base of the liquid column has continuously reduced its diameter, the uplifting effect of the capillary wave at its top further thins the liquid column. This is the first stage of partial coalescence. In the second stage, the column becomes sufficiently thin for capillary instability to set in. A neck forms near the base of the column and eventually a daughter drop pinches off. The mechanism of this pinchoff is analogous to that operating in the capillary instability of a thread.<sup>2,6,7</sup> Unlike in Charles and Mason,<sup>2</sup> we have never observed satellite drops.

Guided by the above understanding, we can derive scal-

TABLE I. Fluid combinations used in our experiments. The percentages are by volume, the densities are in  $\text{g}/\text{cm}^3$ , the viscosities are in centipoise, and the interfacial tensions are in  $\text{dyn}/\text{cm}$ . All experiments are done at  $20^\circ\text{C}$ .

Ambient fluid decane + % polybutene	Drop fluid water + % glycerol	$\rho_1$	$\rho_2$	$\mu_1$	$\mu_2$	$\sigma$	Symbols
0	0	1.0	0.73	1.0	1.0	32.0	◊
20	0	1.0	0.76	1.0	2.0	29.7	○
40	0	1.0	0.79	1.0	5.1	23.7	+
0	20	1.06	0.73	2.1	1.0	37.0	□
0	33	1.10	0.73	3.4	1.0	32.0	◆

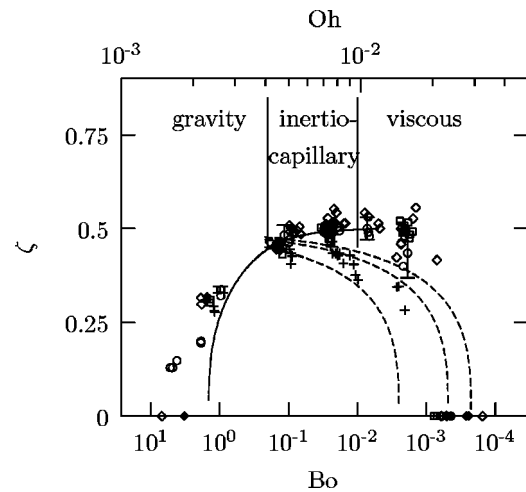


FIG. 3. The drop-size reduction ratio as a function of  $Bo$  and  $Oh$ . The symbols are the same as in Fig. 2. The solid line corresponds to Eq. (6), while the dashed lines are Eq. (4) with three values of  $\mu_*$ . Top curve:  $\mu_*=1$  (diamonds); middle:  $\mu_*=0.5$  (circles); bottom:  $\mu_*=0.196$  (pluses).

ing relations for  $\tau_c$  and  $\zeta$  in each of the three regimes. We will analyze  $\tau_c$  first. In the self-similar regime, both gravity and viscosity are negligible, and the dynamics is dominated by the balance between capillarity and inertia. The only time scale is the capillary time  $t_c$  required for the capillary wave to traverse the length  $D$ ,

$$t_c = \sqrt{\frac{\bar{\rho}D^3}{\sigma}}, \quad (1)$$

where  $\bar{\rho}=(\rho_1+\rho_2)/2$ . Thus the coalescence time scales with  $t_c$  in this regime, as is evident in Fig. 2. The only nondimensional parameter in this case is the density ratio  $\rho_*$ . In the modest range ( $1.26 \leq \rho_* \leq 1.51$ ) covered here, all data obey the same scaling. This extends the previous work of

Thoroddsen and Takehara<sup>3</sup> that deals with very large  $\rho_*$  values only.

For larger drops, the Bond number is larger and gravity may play an important role. Figures 2 and 3 already show the qualitative effect of gravity in helping drainage of the drop and shortening the coalescence times in comparison to the inertia-capillary regime. A modified time scale can be derived by considering the time required for gravity-capillary waves of small amplitude to traverse the length  $D$ ,

$$t_{cg} = \frac{t_c}{\sqrt{1+Bo}}, \quad (2)$$

which is equal to  $t_c$  for small  $Bo$  and to the gravitational time scale  $t_g=\sqrt{\bar{\rho}D/(\rho_1-\rho_2)g}$  for large  $Bo$ . This time scale describes the coalescence time quite well in the self-similar and the gravitational regimes; a best fit  $\tau_c=0.77t_{cg}$  is plotted in Fig. 2. Since inertia is appreciable in the coalescence process, an additional dependence on  $\rho_*$  is possible. Thus, it is somewhat surprising to see the dependence of the time scale on the two densities to be described by Eq. (2). Notice in Fig. 2 that the data sets that collapse to a single curve include our own data for various fluid combinations as well as data of Thoroddsen and Takehara.<sup>3</sup>

For smaller drops, viscosity plays an important role in delaying the pinchoff and thus assisting complete merging. We find that the change in wave speed due to viscosity accounts for less than 5% of the increase in  $\tau_c$  for small drops. Thus, viscosity seems mostly to delay the second stage of the process, i.e., pinchoff. If we assume an effective filament diameter  $\epsilon D$ , the time scale for viscous capillary pinchoff is<sup>6,7</sup>

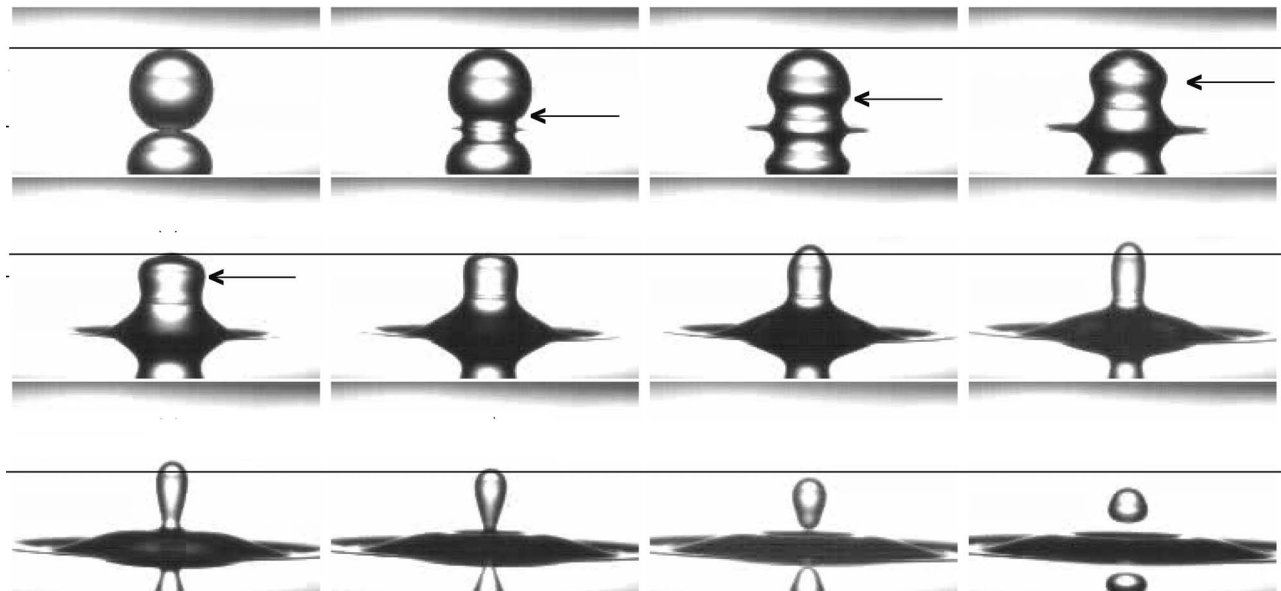


FIG. 4. Snapshots of a water droplet merging with an interface between 20% polybutene in decane and water. The initial drop diameter  $D=1.1$  mm,  $Bo=9.59 \times 10^{-2}$ ,  $Oh=4.17 \times 10^{-3}$ , and the pictures are  $542 \mu s$  apart in time. The location of the capillary wave is shown by the arrows. The horizontal lines, which are at the same height in all three rows, help in tracking the motion of the top of the drop.

$$t_{cv} = t_c \left( 1 + \frac{3 + \mu_*^{-1}}{\sqrt{\epsilon}} \text{Oh} \right). \quad (3)$$

Compared with the data in Fig. 2, Eq. (3) correctly predicts the upward trend with increasing Oh. But the scatter in the data obscures the effect of  $\mu_*$ . As an example, the dashed line in Fig. 2 shows a fitting of the pluses ( $\mu_*=0.196$ ) with  $\epsilon=0.70$  that is determined next from fitting the drop-size reduction ratio  $\zeta$ .

In all three regimes,  $\zeta$  depends on the amount of fluid that drains out of the drop in the coalescence time  $\tau_c$ . The forces that drive and resist the drainage vary from regime to regime. In the viscous regime, we assume that the characteristic velocity for drainage is given by the capillary velocity  $U_c = \sqrt{\sigma/\rho_1 D}$ , while the coalescence time is given by Eq. (3). Then the volume drained from the drop is approximated by  $t_{cv} U_c (\epsilon D)^2$ , which leads to an expression for the drop size ratio  $\zeta$  in terms of  $\epsilon$ ,  $\mu_*$ , and Oh. While the  $\tau_c$  data are too noisy to yield a value for  $\epsilon$  from fitting Eq. (3),  $\epsilon$  can now be determined by the constraint that  $\zeta$  recovers the plateau value  $\zeta_c \approx 0.5$  in the self-similar regime for  $\text{Oh}=0$ :  $\epsilon = [\pi/6(1 - \zeta_c^3)]^{1/2} (\rho_1/\bar{\rho})^{1/4} \approx 0.70$  for all the fluid combinations. Then we have

$$\zeta = \zeta_c \left[ 1 - \frac{3 + \mu_*^{-1}}{\sqrt{\epsilon}} \frac{1 - \zeta_c^3}{\zeta_c^3} \text{Oh} \right]^{1/3}. \quad (4)$$

For the top three fluid pairs in Table I, this model is depicted in Fig. 3. Although the agreement with measured  $\zeta$  is poor, except perhaps for the most viscous matrix (pluses), Eq. (4) does capture, with no fitting parameters, the correct trends that  $\zeta$  decreases with Oh and increases with  $\mu_*$ . It also gives reasonable predictions for the critical Oh where  $\zeta$  drops to zero.

In the gravitational regime, we use a similar argument where the time scale is  $t_{cg}$  and the velocity scale  $U_{cg}$  is given by the Bernoulli equation,

$$\frac{1}{2} \rho_1 U_{cg}^2 = \frac{4\sigma}{\epsilon D} + b(\rho_1 - \rho_2)gD, \quad (5)$$

where the constant  $b$  accounts for the fact that in this complex process, the importance of each term may not be exactly the same as in Bernoulli's equation. Requiring  $\zeta = \zeta_c$  at  $\text{Bo} = 0$  gives  $\epsilon \approx 0.284$ . Thus we obtain

$$\zeta = \left[ 1 - 0.875 \sqrt{\frac{1 + 0.071b\text{Bo}}{1 + \text{Bo}}} \right]^{1/3}. \quad (6)$$

The best fit at  $b=21.1$  is compared with experimental data in the gravity regime in Fig. 3. The model predicts a critical  $\text{Bo}=1.58$  for the largest drop to have partial coalescence, smaller than measured values.

Based on the analysis above, partial coalescence takes place when pinchoff occurs before the drop fluid has time to drain completely. Therefore, the critical conditions consist in a maximum Bo for large drops and a maximum Oh for small drops. Figure 5 depicts a crude "phase diagram" for partial and complete coalescence for the fluid combinations used in

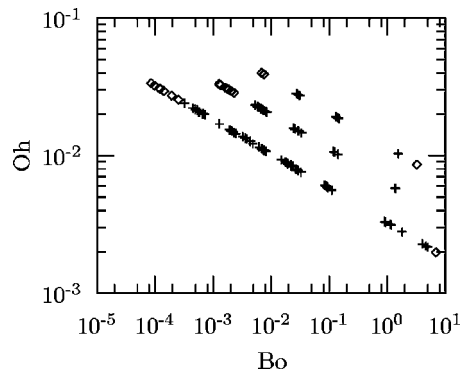


FIG. 5. A phase diagram for partial coalescence. Pluses indicate partial coalescence while diamonds complete merging. The data for each fluid combination form straight lines:  $\text{Bo}\text{Oh}^4 = \text{const}$ . The topmost line corresponds to water+33% glycerol in decane, the middle line water+20% glycerol in decane, and the bottom line consists of three data sets for water in decane, decane+20% polybutene, and decane+40% polybutene.

our experiments. Mohamed-Kassim and Longmire<sup>4</sup> postulated a different criterion for partial coalescence,  $\text{Bo}\text{Oh} < 0.02-0.03$ . Our observations and analysis do not support a criterion based on  $\text{Bo}\text{Oh}$ , and we have observed complete coalescence for a much lower  $\text{Bo}\text{Oh} = 3.19 \times 10^{-6}$ .

In closing, we point out that our analysis concerns mostly low-viscosity fluids. Note that  $\text{Bo}\text{Oh}^4$  scales with  $\mu_1^4$ . As the drop phase gets more viscous, it soon becomes impossible for Bo and Oh to be small simultaneously. Then the inertia-capillary regime will be eliminated, and viscosity will have a role even for large drops. This may explain the different criteria for partial coalescence noted above. Indeed, gravity, capillarity and viscosity are all important in the partial coalescence scenarios that Mohamed-Kassim and Longmire<sup>4</sup> analyzed. In addition, we have ignored any surfactant effects. While reasonable attempts were made to maintain the purity of the fluids, the measured surface-tension values were sometimes lower than those in handbooks, perhaps due to impurities. This may be partly responsible for the noisy data in the viscous regime.

This work was supported by the Petroleum Research Fund, the Canada Research Chair Program, the NSERC, and the Canada Foundation for Innovation. We thank Siddharth Khullar for assistance with the experiment.

<sup>1</sup>G. E. Charles and S. K. Mason, "The coalescence of liquid drops with flat liquid/liquid interfaces," *J. Colloid Sci.* **15**, 236 (1960).

<sup>2</sup>G. E. Charles and S. K. Mason, "The mechanism of partial coalescence of liquid drops at liquid/liquid interfaces," *J. Colloid Sci.* **15**, 105 (1960).

<sup>3</sup>S. T. Thoroddsen and K. Takehara, "The coalescence cascade of a drop," *Phys. Fluids* **12**, 1265 (2000).

<sup>4</sup>Z. Mahamed-Kassim and E. K. Longmire, "Drop coalescence through a liquid-liquid interface," *Phys. Fluids* **16**, 2170 (2004).

<sup>5</sup>S. T. Thoroddsen, K. Takehara, and T. G. Etoh, "The coalescence speed of a pendant and a sessile drop," *J. Fluid Mech.* **527**, 85 (2005).

<sup>6</sup>S. Tomotika, "On the instability of a cylindrical thread of a viscous liquid surrounded by another viscous fluid," *Proc. R. Soc. London, Ser. A* **150**, 322 (1935).

<sup>7</sup>C. M. Kinoshita, H. Teng, and S. M. Masutani, "A study of the instability of liquid jets and comparison with Tomotika's analysis," *Int. J. Multiphase Flow* **20**, 523 (1994).